

Hydrodynamic and Mass Transfer Properties in a Three Phase External Loop Airlift Compared with a Three Phase Internal Loop Airlift and a Slurry Bubble Column

K. Nakao⁺, S. Suenaga, K. Furumoto*, M. Yoshimoto, and K. Fukunaga

Department of Applied Chemistry and Chemical Engineering,
Yamaguchi University, Tokiwadai, Ube, Yamaguchi 755-8611, Japan;
e-mail: knakao@yamaguchi-u.ac.jp

*Oshima National College of Maritime Technology, Oshima,
Yamaguchi 742-2106, Japan

Original scientific paper
Received: May 29, 2007
Accepted: October 15, 2007

The effects of suspended solid particles on the hydrodynamic and mass transfer properties were experimentally studied in a wide range of the superficial gas velocity, solid particle property and liquid viscosity in an external loop airlift bubble column in comparison with those in an internal loop airlift bubble column as well as a normal bubble column. The circulating liquid velocities U_L , gas holdups ε_G and volumetric gas liquid oxygen transfer coefficients $k_L a$ in the riser of the external loop airlift were found to be almost unaffected by the completely suspended solid particles. The above three properties obtained could be represented by our previous correlations for the gas-liquid two phase flow within an accuracy of $\pm 30\%$ for a practical reactor design and operation. The analogous results were obtained on the ε_G and $k_L a$ data in the three phase normal and internal loop airlift bubble columns, although a small amount of suspended solid particles was observed to cause a slight decrease in these values in contrast to a lower or negligible decrease in those of the three phase external loop airlift.

Key words:

External loop airlift, internal loop airlift, normal bubble column, three phase flow, suspended solid particles, circulating liquid velocity, gas holdup, volumetric oxygen transfer coefficient

Introduction

Much work has been done on the hydrodynamics and mass transfer in the gas-liquid two phase flow in the external loop airlift bubble column (ELBC).¹⁻³ The unique feature of ELBC is its well-defined recirculating liquid flow pattern which makes the hydrodynamic and mass transfer properties different from those in the internal loop airlift bubble column (ILBC) and normal bubble column (NBC). Especially, the liquid circulation makes the solid particle loading more uniformly suspended in ELBC than in either ILBC or NBC. Recently, more attention has been paid to the gas-liquid-solid three phase flow in ELBC.⁴⁻⁶ However, effects of suspended solid particles on the hydrodynamic and mass transfer properties have not fully been clarified because of a complicated interaction between bubbles, liquid and solid particles even in ELBC.

The purpose of this work is to (a) measure the effects of suspended solid particles on the circulating liquid velocity U_L , gas holdup ε_G and volumetric gas-liquid oxygen transfer coefficient $k_L a$ in the riser of ELBC, (b) compare the ε_G and $k_L a$ values

with those in ILBC and NBC in a wide range of the superficial gas velocity U_G , solid particle properties and liquid viscosity to discuss the bubbles flow behavior in view of bubble coalescence and breakup and (c) examine the applicability of our previous correlations for the two phase flow in each column to correlate the properties in the three phase flow for a practical reactor design and operation.

Experimental

The apparatus used was almost the same as in our previous work on the gas-liquid two phase flow.² Fig. 1(a) shows a schematic diagram of the ELBC. As is shown in Fig. 1(b), the ILBC had a draft tube of 5 cm in diameter with gas injection into the annular section. The ILBC was used as the NBC by removing the draft tube. Table 1 summarizes the experimental conditions. The superficial gas velocity U_G in the ELBC was defined based on the cross sectional area of the riser and the velocity in the ILBC was on the column cross sectional area in the same way as that in the NBC. The U_G values employed were 0.02, 0.04, 0.08, 0.16 and 0.32 cm/s throughout the present experimental work.

⁺Corresponding author

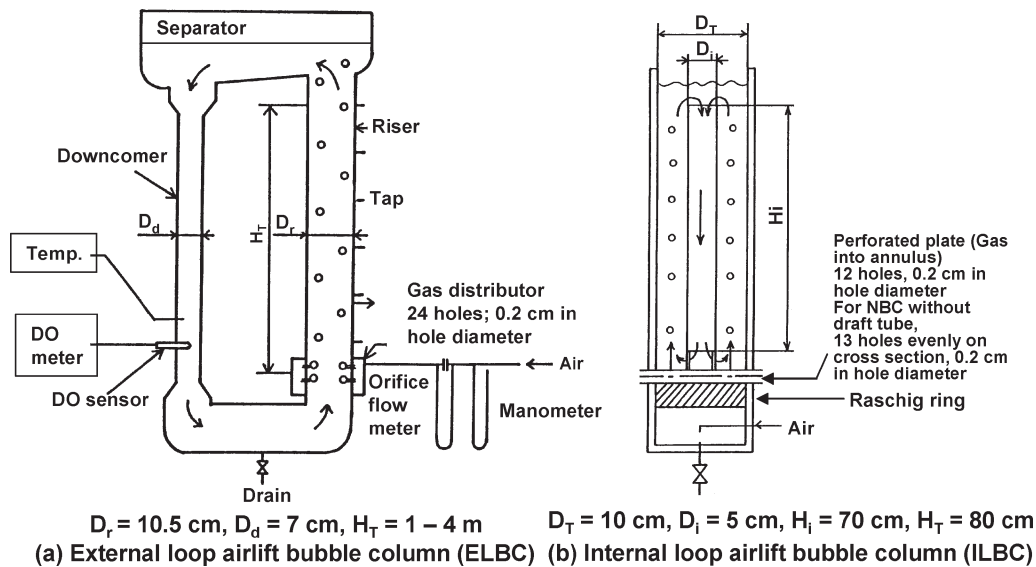


Fig. 1 – Schematic diagram of experimental apparatus

Table 1 – Experimental conditions

Gas: Air, Nitrogen, Superficial gas velocity $U_G = 0.02 \sim 0.32$ m/s

Liquid: Tap water, aq. 0.5-2.0 wt% CMC soln. (Pseudo-plastic fluid, $\mu_a = K \cdot \gamma^{n-1}$)

Static liquid height $H_T = 1 \sim 4$ m (ELBC), 0.8 m (ILBC, NBC)

Solid: Ion exchange resin (IR) ($d_p = 450, 910 \mu\text{m}$, $\rho_s = 1252 \text{ kg/m}^3$),

Glass beads (GB) ($d_p = 710, 940 \mu\text{m}$, $\rho_s = 2500 \text{ kg/m}^3$)

Solid concentration, $C_S = 0.01 \sim 0.20 \text{ kg/dm}^3$ -slurry

Temp.: 298–300 K

The values of $k_L a$ were obtained by carrying out both the desorption of dissolved oxygen into nitrogen gas flow and the absorption of oxygen in air flow into the aqueous phase in the column. The time course of the dissolved oxygen was measured with a dissolved oxygen electrode inserted in the liquid phase through the column wall as shown in Fig. 1(a). The liquids used were tap water and aqueous 0.5 to 2.0 % carboxymethyl cellulose (CMC) solutions. CMC was used to increase the liquid viscosity. The time course measured simultaneously at the top of the riser in the ELBC agreed with the one at the bottom of the downcomer, suggesting that the liquid phase was well mixed in the ELBC with respect to the process. A high recirculating liquid flow rate in the batch liquid phase was considered to support the above mixing state. Negligible effect of the dissolved oxygen electrode response time on the time course was safely assumed due to the relatively low values of $k_L a$ of less than 0.1 s^{-1} .⁷ This requirement for the electrode was more easily satisfied in the ELBC than in the ILBC and NBC because the former had the bubble free liquid volume

consisting of the downcomer column top and bottom. The volume contributed to diluting the instantaneous dissolved oxygen concentration and reducing the rate of its change in the ELBC. The ratio of the bubble free liquid volume to the liquid volume in the riser was about 2 and 1 for the static liquid height H_T of 1 m and 4 m, respectively under the condition of $U_G = 0$. To prevent bubbles from recirculating through or residing in the downcomer, a sufficient liquid volume was provided in the gas-liquid separation section at the column top.

The gas holdup ε_G in the riser of the ELBC was determined from an analysis of the gradient of static pressure along the column height considering the pressure due to suspended solid particles. The values of ε_G in the ILBC and NBC were measured by the volume expansion method. The above methods for measuring the ε_G value in the whole column are considered to be useful and reliable for such a bench or pilot scale column as in this work.

The circulating superficial liquid velocity U_L in the three phase flow through the riser was measured

in the same way as in the two phase flow in our previous work² using a plastic sphere of 1.2 cm diameter having the same density as the liquid phase in the downcomer almost free of gas bubbles. The reliable value of U_L was obtained by averaging the U_L values for 20 times measurements under each experimental condition. The velocity in the downcomer was multiplied by the ratio of downcomer cross sectional area A_d to riser one A_r to obtain the U_L value.

The rheological properties of the CMC solutions were measured at 298 K with a concentric cylinder viscometer to determine the apparent liquid viscosity $\mu_a = K\dot{\gamma}^{n-1}$ according to the power law model. The values of both the fluid consistency index K and the flow behavior index n were reported in our previous paper.² The $k_L a$ values were measured at room temperature (293 to 300 K) in the case of water without CMC. The temperature of CMC solution in the taller ELBC was kept at almost constant of 298 K by a temperature controller unit installed in the gas-liquid separator. Triplicate experimental data on either of U_L , ε_G or $k_L a$ were within a standard deviation of $\pm 5\%$ of each mean value.

Calculation of volumetric transfer coefficient $k_L a$

The $k_L a$ values for the riser were determined considering that the liquid phase was well mixed in the whole column as described above, the gas phase passed through the riser in plug flow⁸ and negligible oxygen transfer occurred in the downcomer because of almost complete separation of gas from liquid at the top of the ELBC operated in such a way as mentioned before.

The progressive change of the dissolved oxygen concentration C_O is derived as follows⁹

$$\ln \left\{ \frac{(HP_b - C_O)}{(HP_b - C_O^0)} \right\} = -k_L a_L t \quad (1)$$

where $k_L a_L$ is the coefficient per unit volume of the liquid in the whole column, H the Henry's law constant and P_b the oxygen partial pressure at the column bottom. Thus, the slope of a linear plot of the left-hand side term of Eq. (1) vs. t gives the values of $k_L a_L$. This value of $k_L a_L$ is a result of an instantaneous mixing or dilution of the dissolved oxygen in the riser with that in downcomer due to a sufficiently high recirculating liquid flow rate through the whole column. $k_L a_L$ is, therefore, converted to $k_L a$, the coefficient per unit volume of the gas-liquid-solid dispersion in the riser.

$$k_L a = k_L a_L (1 - \varepsilon_G - \varepsilon_S) (1 + V_d/V_r) \quad (2)$$

where V_d and V_r are the liquid volumes in the downcomer and riser, respectively and $\varepsilon_S = (1 - \varepsilon_G)C_S/\rho_S$ is the solid holdup calculated from the initial solid loading C_S [kg solid/m³ slurry]. V_d includes the bubble free liquid volumes at both column top and bottom.

The $k_L a_L$ values for the ILBC and NBC are also determined according to Eq. (1) and then reduced into the values of $k_L a$ using Eq. (2) with $V_d = 0$.

Results and discussion

Effects of solid particle loading and properties on U_L , ε_G and $k_L a$ in three phase ELBC

The effects of the density ρ_S , mean diameter d_p and loading C_S of solid particles on U_L , ε_G and $k_L a$ in the three phase ELBC were examined as a function of U_G with tap water and $H_T = 1$ m in comparison with those in the two phase ELBC. Furthermore, the results on the ε_G and $k_L a$ values were compared with those in the three and two phase ILBC and NBC.

Fig. 2 shows the results on U_L in ELBC. The solid line in the figure is the result calculated from the previous correlation Eq. (3a) as shown in Table 2 where the other correlations for the two phase ELBC, ILBC and NBC are listed.² These correlations were reported to reproduce the observed values of U_L , ε_G and $k_L a$ with an error of $\pm 20\%$. It should be noted in the figure that no standard deviation can be shown for each key as its height is almost the same as the bar height corresponding to

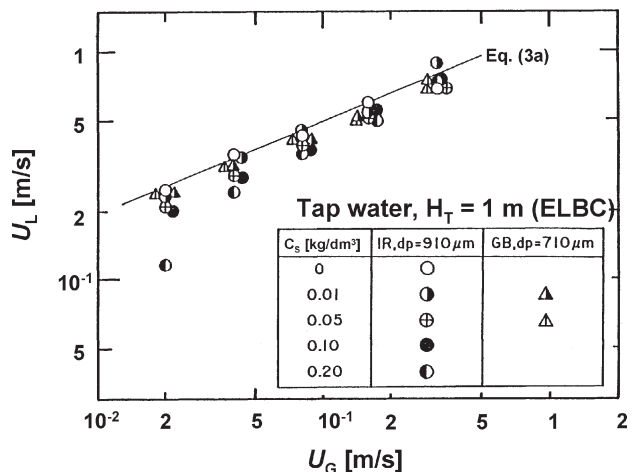


Fig. 2 – Effect of superficial gas velocity U_G and solid loading C_S on circulating liquid velocity U_L in riser of ELBC with static liquid height H_T of 1 m. The liquid was tap water at 298–300 K. The viscosity was $0.89 \times 10^{-3} \text{ Pa} \cdot \text{s}$ at 298 K. The measurements were made at U_G values of 0.02, 0.04, 0.08, 0.16 and 0.32 m/s. The solid particles used were ion exchange resin IR and glass beads GB of diameter $d_p = 910 \mu\text{m}$ and $710 \mu\text{m}$, respectively. The C_S values were varied from 0 to 0.20 kg/dm³ as shown in the figure.

Table 2 – Correlations for U_L , ε_G and $k_L a$ in gas-liquid system using μ_a^2

ELBC	$U_L = 1.84 (A_d/A_T)^{0.75} U_G^{0.40} \mu_a^{-0.030} H_T^{0.31}$	$(\mu_a \leq 0.04$	(3a)
	$U_L = 0.23 (A_d/A_T)^{0.75} U_G^{0.40} \mu_a^{-0.675} H_T^{0.31}$	$\text{Pa} \cdot \text{s})$	(3b)
ELBC	$U_G/\varepsilon_G = \{0.43 + 2.00 (U_G + U_L)\} \mu_a^{0.082}$	$(\mu_a \leq 0.04)$	(4a)
	$U_G/\varepsilon_G = \{0.68 + 3.40 (U_G + U_L)\} \mu_a^{0.26}$	$(\mu_a > 0.04)$	(4b)
ILBC, NBC	$U_G/\varepsilon_G = 0.53 \mu_a^{0.11} + 2.4 U_G$		(5)
ELBC	$k_L a = 8.09 \times 10^{-2} \varepsilon_G^{1.2} \mu_a^{-0.35}$	$(\mu_a \leq 0.04)$	(6a)
	$k_L a = 1.97 \times 10^{-2} \varepsilon_G^{1.2} \mu_a^{-0.79}$	$(\mu_a > 0.04)$	(6b)
ILBC, NBC	$k_L a = 4.80 \times 10^{-2} \varepsilon_G^{1.1} \mu_a^{-0.28}$	$(\mu_a \leq 0.04)$	(7a)
	$k_L a = 1.53 \times 10^{-2} \varepsilon_G^{1.1} \mu_a^{-0.63}$	$(\mu_a > 0.04)$	(7b)

$\mu_a = K\gamma^{m-1}$ where $\gamma = 5000 U_G$ according to Nishikawa et al. (1977)¹⁰

the upper limit of the standard deviation equal to $\pm 5\%$ of the mean value of each key in the logarithmic scale. Furthermore, some of the keys very close to each other at a fixed value of U_G are seen to be plotted against the U_G value near the fixed U_G . Such a graphic representation of data as above is applied to the other data which are shown in the following. It is seen in the figure that the higher U_G gives the higher U_L and thus at the U_G value higher than 5 m/s, the solid loading C_S exerts negligible effect on U_L for either ion exchange resin (IR) particles or glass beads (GB) although a slight but an undefined decrease is observed with increasing C_S at a given U_G . The decrease in U_L with increasing C_S is more remarkable at a lower U_G less than 0.05 m/s for the IR particles. The lowest U_L value is seen to be observed at the lowest U_G of 0.02 m/s and highest C_S of 0.20 kg/dm³ for the IR particles. This is probably because the IR particles were visually observed to be concentrated along the horizontal bottom of ELBC, which reduced the cross sectional area available for the liquid flow and decreased U_L . A comparison of the U_L values for two C_S values of 0.01 and 0.05 kg/dm³ at any fixed U_G value reveals that the GB exerts a smaller influence on U_L than the IR particles. This may be because the former has two times greater density and hence the lower (a half) solid holdup ε_S in the three phase flow compared to the latter. Due to the difficulty in determining a slight but an undefined dependence of U_L on the C_S and solid particle properties as described above, the dependence was regarded as negligible provided that almost all of the solid particles loaded initially were suspended and recirculated through the whole column. Therefore, the U_L values were concluded to be approximately correlated by Eq. (3a) for the two phase ELBC for the purpose of a practical reactor design and operation.

Fig. 3 shows the results on ε_G in ELBC and ILBC. The results on NBC agreed well with those in ILBC. The upper and lower solid lines are from the correlations Eq. (4a) for two phase ELBC and Eq. (5) for two phase ILBC and NBC in Table 2. The ε_G value for $U_G = 0.02$ m/s and $C_S = 0.20$ kg IR/dm³ in the three phase ELBC is seen to be close to that in the two phase ELBC in contrast to the U_L value mentioned above. This suggests that ε_G is unaffected by inhomogeneous distribution of solid particles in ELBC. For U_G higher than 0.05 m/s, ε_G in any bubble column is seen to be almost unaffected by the suspended solid particles. For the lower U_G , the reduction in ε_G due to solid particles seems to be slightly greater in ILBC and NBC than in ELBC. This is due to the fact that the higher lo-

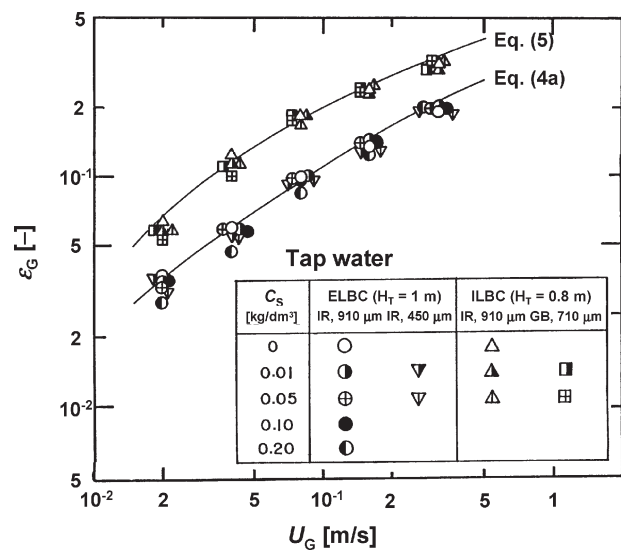


Fig. 3 – Effect of U_G and C_S on gas holdup ε_G in riser of ELBC with H_T of 1 m and on ε_G in ILBC with $H_T = 0.8$ m. The operating conditions were the same as those shown in Fig. 2 except for use of 450 μm IR instead 710 μm GB in ELBC.

cal solid particles concentrations at the lower part of ILBC and NBC tends to enhance the bubble coalescence generating the larger bubbles. Due to a very slight difference in ϵ_G between the three and two phase bubble columns of any type, ϵ_G in any type of three phase bubble column can be represented by the correlation of ϵ_G for the corresponding two phase column.

Figs. 4(a) and 4(b) show the results on $k_L a$ in ELBC and those in ILBC and NBC, respectively. The solid lines in the two figures are from the cor-

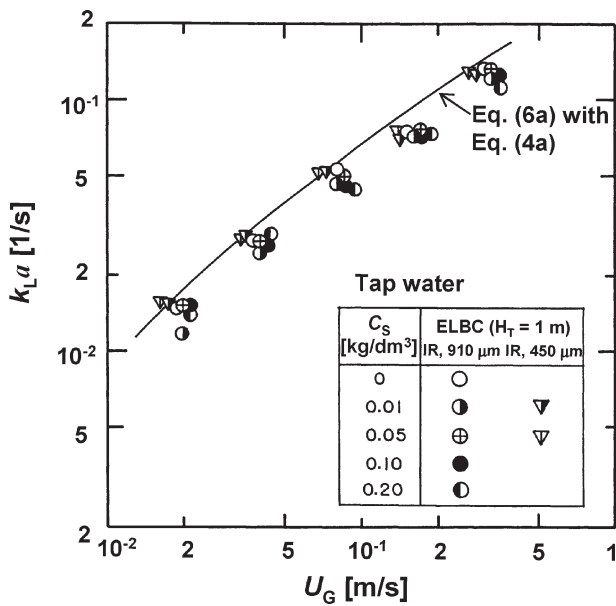


Fig. 4 (a) – Effect of U_G and C_s on volumetric gas-liquid oxygen transfer coefficient $k_L a$ based on dispersion volume in riser of ELBC with $H_T = 1$ m. The operating conditions were the same as those shown for ELBC in Fig. 3.

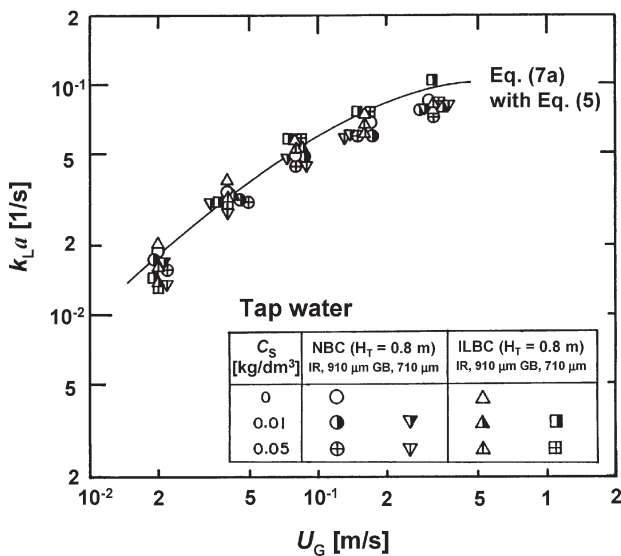


Fig. 4 (b) – Effect of U_G and C_s on $k_L a$ based on dispersion volume in both ILBC and NBC with the same H_T of 0.8 m. The operating conditions were the same as those shown for ILBC in Fig. 3.

relations Eq. (6a) with Eq. (4a) for two phase ELBC and Eq. (7a) with Eq. (5) for two phase ILBC and NBC in Table 2. Almost no effects of the solid loading and properties on $k_L a$ are suggested in ELBC according to Fig. 4(a) since the particles tend to be completely and uniformly suspended by a high U_L except for the condition of $U_G = 0.02$ m/s and $C_s = 0.20$ kg IR/dm³ and thus to reduce the bubble coalescence compared to those in ILBC and NBC. Due to very slight, but an undefined dependence of $k_L a$ on the solid particle loading and properties, the $k_L a$ values in three phase ELBC were proposed to be correlated by Eq. (6a) with Eq. (4a) for two phase ELBC. Based on the results shown in Fig. 4(b), on the other hand, because of the higher local solid particles concentrations near the gas distributor in ILBC and NBC, a frequent bubble coalescence is suggested to generate the larger bubbles resulting in a decrease in the gas-liquid interfacial area a and hence a decrease in $k_L a$. The dependence of $k_L a$ in ILBC and NBC on the solid particle loading and properties is seen to be slightly greater than that of $k_L a$ in ELBC, although the former dependence is still very slight and undefined. Therefore, the $k_L a$ values in three phase ILBC and NBC were suggested to be correlated by Eq. (7a) with Eq. (5) for two phase ILBC and NBC. Comparison of Figs. 4(a) and 4(b) reveals that $k_L a$ in ELBC increases steadily with increasing U_G while $k_L a$ in ILBC and NBC tends to be flattened with increasing U_G . This is due to the fact that the higher circulating liquid velocity at the higher U_G contributes to a reduction in bubble coalescence frequency. Whereas ELBC has the lower ϵ_G than ILBC and NBC as shown in Fig. 3, ELBC exceeds the $k_L a$ value in ILBC and NBC at U_G greater than 0.1 m/s as seen from Figs. 4(a) and 4(b).

Figs. 5(a) and 5(b) show the ϵ_G and $k_L a$ values, respectively, as a function of C_s or ϵ_s with U_G , column type, particle diameter and density as parameters. The literature data on ILBC¹¹ and NBC¹² are also shown for comparison. It is seen from the figures that (1) both ϵ_G and $k_L a$ in ELBC are almost unaffected by C_s in a wide range of $C_s = 0 \sim 0.2$ kg/dm³, (2) ϵ_G even in ILBC and NBC including the literature data is only a little influenced by the solid particle loading, while $k_L a$ in ILBC and NBC remarkably depends on the loading and (3) the dependence of $k_L a$ on the particle loading may be limited to a very low C_s being less than 0.05 kg/dm³ according to the present data. The last observation suggests that a minimum amount of solid particles may suffice to exert their maximum effect on the bubble coalescence and breakup governing the mean bubble size. It was previously reported that the effect of solid particle loading was important for small

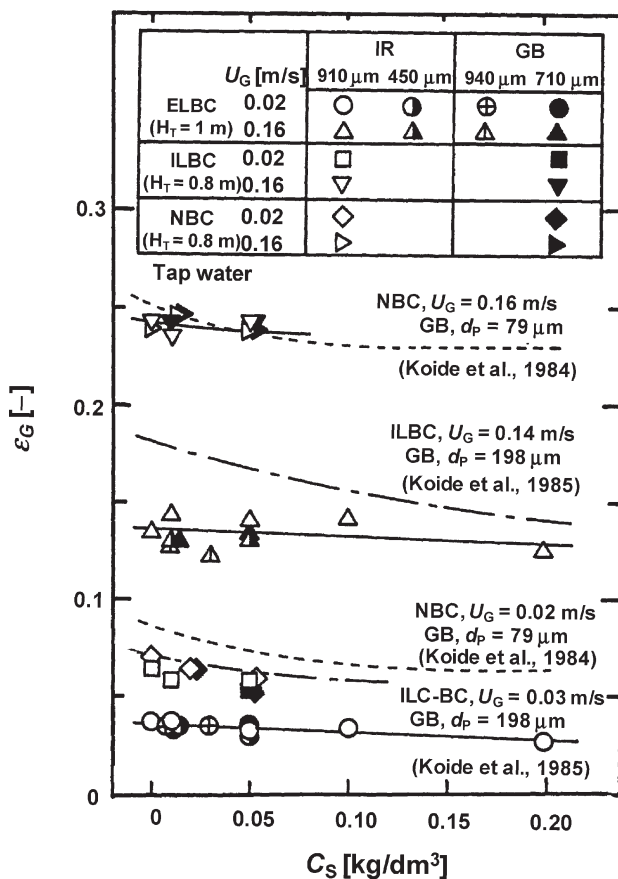


Fig. 5 (a) – ε_G as a function of C_s at fixed U_G values of 0.02 and 0.16 m/s in ELBC with $H_T = 1$ m compared with ε_G in ILBC and NBC with the same $H_T = 0.8$ m as well as ε_G in the literature. The measurements were made at C_s values of 0 (tap water), 0.01, 0.05, 0.10 and 0.20 kg/dm³. The liquid was tap water at 298-300 K. Two different sizes of IR and GB were used as shown in the figure.

values of C_s (up to 5 % w/v) due to enhanced bubble coalescence, mainly controlling the interfacial area a .¹³

Effects of static liquid height and liquid viscosity on U_L , ε_G and $k_L a$ in three phase ELBC

The effects of static liquid height H_T and apparent liquid viscosity μ_a (CMC concentration) on U_L , ε_G and $k_L a$ in the three phase ELBC were observed as a function of U_G with the IR particles of $d_p = 910 \mu\text{m}$ and $C_s = 0.05 \text{ kg/m}^3$ in comparison with those calculated from Eqs. (3), (4) and (6) for two phase ELBC in Table 2. Figures 6(a) and 6(b) show the effects on U_L of H_T and μ_a , respectively. The lines are from Eq. (3). For the higher H_T and μ_a , where particles are easier to suspend completely and uniformly, the U_L values observed much better agree with the values calculated for the two phase flow. Analogously, Fig. 7 shows the results on ε_G . Except for the ε_G values in the case of the highest viscosity (2.0 % CMC) and lower U_G , the ε_G values

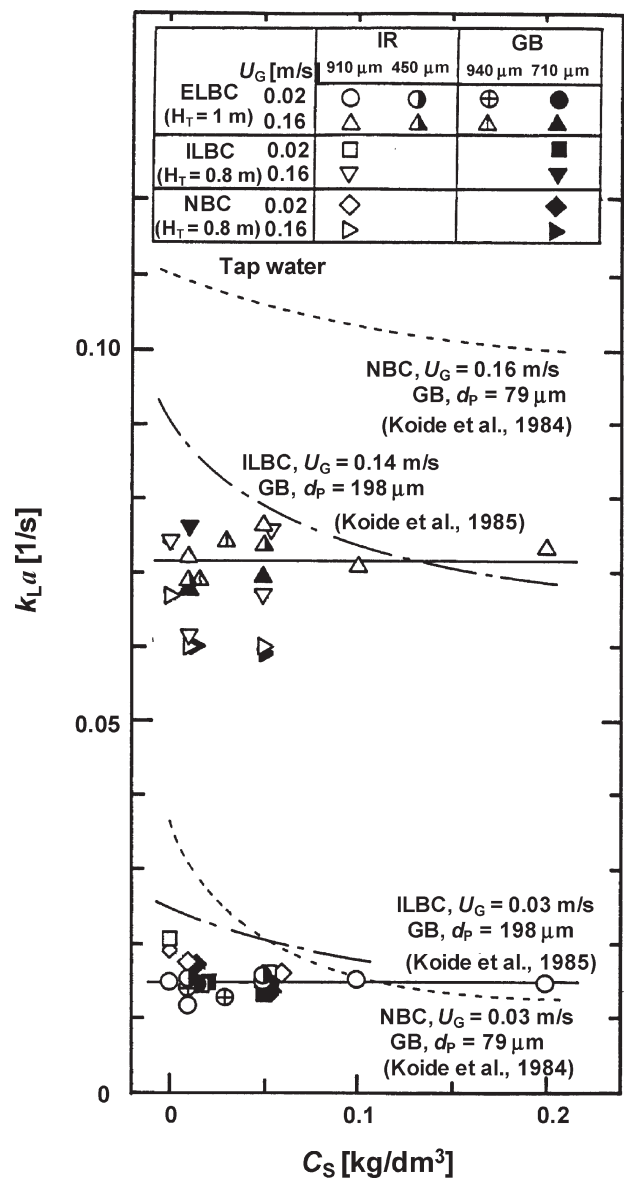


Fig. 5 (b) – $k_L a$ as a function of C_s at fixed U_G values of 0.02 and 0.16 m/s in ELBC with $H_T = 1$ m compared with $k_L a$ in ILBC and NBC with the same $H_T = 0.8$ m as well as $k_L a$ in the literature. The operating conditions were the same as those shown in Fig. 5(a).

observed in the three phase flow are almost equal to those in the two phase one. The too high ε_G values at the lower U_G for the highest viscosity is due to a fully developed slug flow in the riser resulting from the bubble coalescence much more predominant than the breakup in the highly viscous solution.

Fig. 8 shows the results on $k_L a$. The effect of H_T on $k_L a$ shown in Fig. 8(a) is seen to correspond to that on ε_G in Fig. 7(a). On the contrary, the effect of μ_a on $k_L a$ in Fig. 8(b) is much remarkable than that on ε_G in Fig. 7(b). This is because both the mass transfer coefficient k_L and gas-liquid interfacial area a decrease with increasing μ_a .¹⁴ Except for the $k_L a$ values corresponding to the too high ε_G

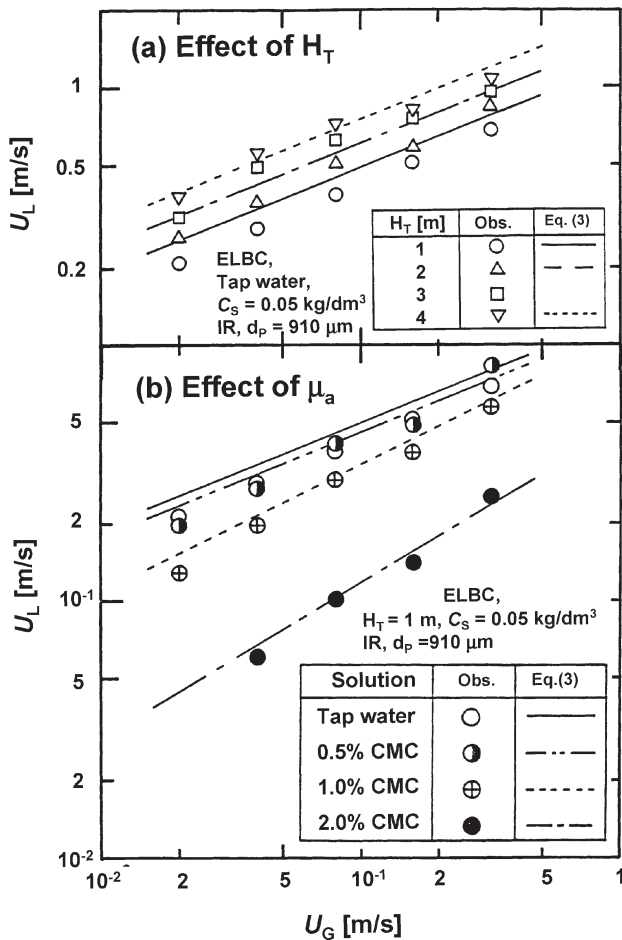


Fig. 6 – Effects of (a) H_T and (b) apparent liquid viscosity μ_a on U_L in riser of ELBC as a function of U_G . U_G was varied from 0.02 to 0.32 m/s in the same way as above. (a) H_T was varied from 1 m to 4 m. C_s was 0.05 kg/dm³ using 910 μm IR. The liquid was tap water at 298–300 K. The lines show the U_L values calculated from Eq. (3) for gas-liquid two phase flow as shown in Table 2. (b) μ_a was varied by using 0% (tap water), 0.5%, 1.0% and 2.0% CMC solution at 298–300 K with the respective μ_a values of 0.89×10^{-3} , $1.6\text{--}1.9 \times 10^{-2}$, $5.0\text{--}7.0 \times 10^{-2}$ and $0.20\text{--}0.50 \text{ Pa} \cdot \text{s}$ depending on U_G value. H_T was fixed at 1 m. The solid loading was the same as that in (a). The lines show the U_L values calculated in the same way as above.

values above, the $k_L a$ values observed are well reproduced by the correlation Eq. (6) with Eq. (4) for the two phase ELBC. A higher value of $k_L a$ in a fully developed slug flow is considered to be due to the same reason as in the case of the superior mass transfer characteristics of Taylor bubble flow in narrow capillaries as in the gas-liquid mass transfer of a monolith loop reactor with upflow of gas and liquid phases through the channels.¹⁵

Correlation of $k_L a$ with ϵ_G for three phase ELBC, ILBC and NBC

Fig. 9 shows a plot of $k_L a$ as a function of ϵ_G using the present data on $k_L a$ and ϵ_G obtained

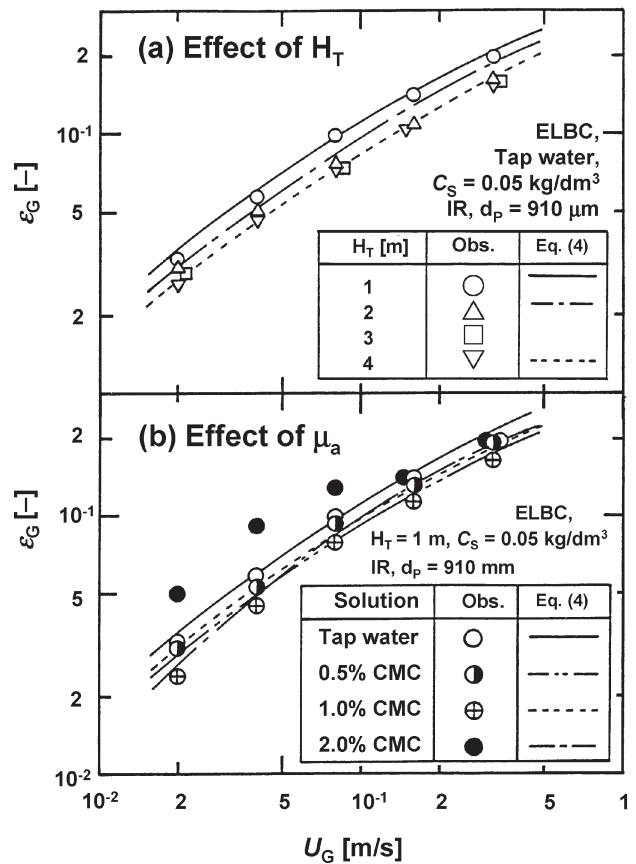


Fig. 7 – Effect of (a) H_T and (b) μ_a on ϵ_G in riser of ELBC as a function of U_G . The variation of U_G and the operating conditions in (a) and (b) were the same as those shown in Fig. 6. The lines show the ϵ_G values calculated from Eq. (4) for two phase flow as shown in Table 2.

in the three phase ELBC, ILBC and NBC with tap water and IR particles (910 μm). It is found from the figure that the $k_L a$ values in the ELBC well agree with Eq. (6a) for the two phase flow and that the $k_L a$ values in the three phase ILBC and NBC also do with Eq. (7a) for the two phase flow and are very close to the correlation of Akita and Yoshida (1973).¹⁶ The $k_L a$ value in ELBC is seen to be higher than that in ILBC and NBC at a fixed value of ϵ_G . This is mainly because the average bubble diameter in ELBC with less bubble coalescence is lower than that in ILBC and NBC.^{17, 18} Figure 10 shows a comparison of the $k_L a$ values observed in three columns with those calculated from the correlations in Table 2 knowing the column geometry, superficial gas velocity and apparent liquid viscosity. Except for the too high observed $k_L a$ values mentioned above, the $k_L a$ values in any three phase columns can be predicted by the correlations for the two phase flow within an accuracy of $\pm 30\%$ being slightly less accurate compared to an accuracy of $\pm 20\%$ in the case of the two phase columns.

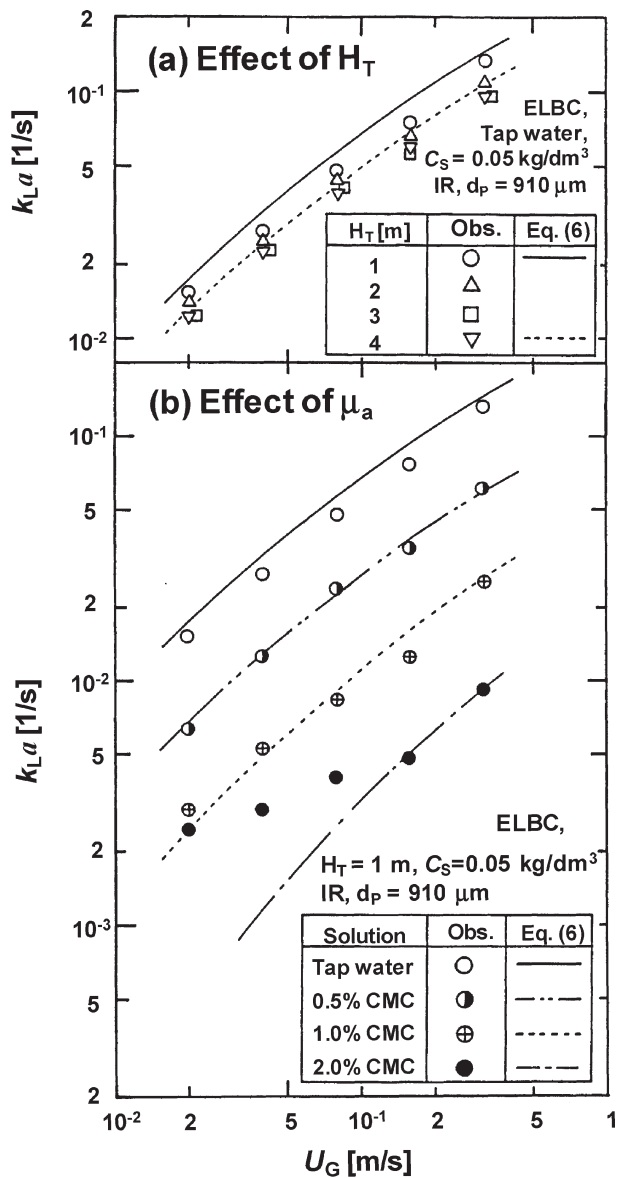


Fig. 8 – Effect of (a) H_T and (b) μ_a on $k_L a$ in riser of ELBC as a function of U_G . The variation of U_G and the operating conditions in (a) and (b) were the same as those shown in Figs. 6 and 7. The lines show the $k_L a$ values calculated from Eq. (6) with Eq. (4) for two phase flow as shown in Table 2.

Conclusion

The effects of suspended solid particles on the hydrodynamic and mass transfer properties were experimentally studied in a wide range of the superficial gas velocity, solid particle property and liquid viscosity in an external loop airlift bubble column in comparison with those in an internal loop airlift bubble column as well as a normal bubble column. The results obtained in this work are summarized as follows.

(1) The solid particles were easier to suspend completely and uniformly in ELBC than ILBC and NBC.

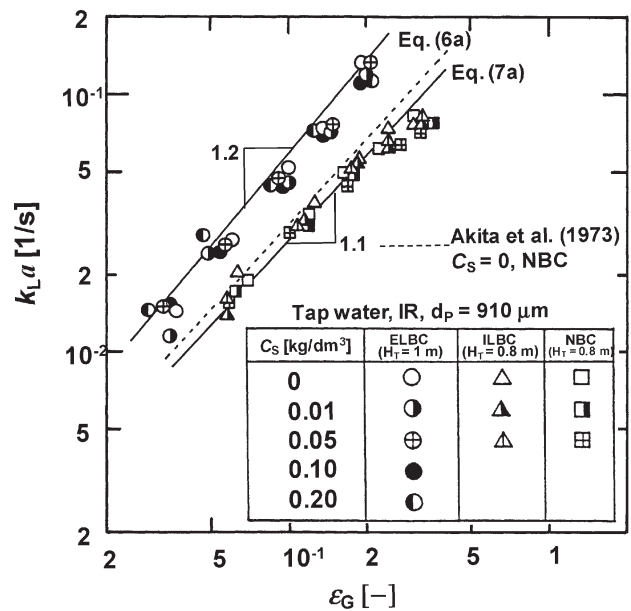


Fig. 9 – Correlation of $k_L a$ with ϵ_G in riser of three phase ELBC compared with corresponding correlations in three phase ILBC and NBC. Ranges of operating conditions were as follows. $U_G = 0.02\text{--}0.32 \text{ m/s}$, 298–300 K, $C_S = 0\text{--}0.20 \text{ kg IR/dm}^3$ tap water and IR was $910 \mu\text{m}$ in diameter. One solid line for ELBC shows the $k_L a$ values calculated from Eq. (6a) for two phase flow as shown in Table 2. The other solid line for ILBC and NBC represents those calculated from Eq. (7a) for two phase flow in both columns as shown in the table. The dotted line is from the literature for two phase NBC.

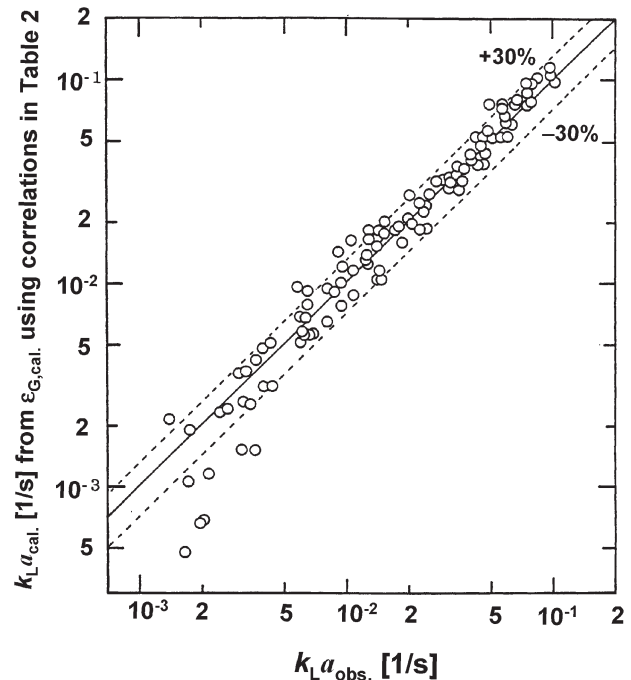


Fig. 10 – Applicability of $k_L a$ -correlations Eqs. (6a), (6b) for two phase ELBC and Eq. (7a), (7b) for either two phase ILBC or NBC to prediction of $k_L a$ values for three phase ELBC and those for either three phase ILBC or NBC, respectively. Ranges of operating conditions were as shown in Table 1. Liquid viscosity of tap water was $0.89 \times 10^{-3} \text{ Pa} \cdot \text{s}$ and the μ_a values of aqueous 0.5 and 2.0 wt% CMC solutions were $1.6\text{--}1.9 \times 10^{-2} \text{ Pa} \cdot \text{s}$ and $0.20\text{--}0.50 \text{ Pa} \cdot \text{s}$, respectively depending on U_G value.

(2) The U_L values in ELBC and the ε_G and $k_L a$ values in ELBC, ILBC and NBC were affected by the suspended solid particles in the case of a significant distribution of particles along column height. In the case of almost complete and uniform distribution of particles, the U_L , ε_G and $k_L a$ values in the three phase flow were only a little affected by the particles and could be represented by our previous correlations for the two phase flow.

(3) A small amount of suspended particles was suggested to exert an effect on the behavior of the gas-liquid interface and hence on the ε_G and $k_L a$ values. Such an effect was easier to observe in ILBC and NBC than in ELBC.

Nomenclature

- a – gas-liquid interfacial area, 1/m
 A_d – cross sectional area of downcomer, m²
 A_r – cross sectional area of riser, m²
 C_O – dissolved oxygen concentration, kmol/m³
 C_O^0 – initial dissolved oxygen concentration, kmol/m³
 C_S – solid particle concentration based on bubble free volume, kg/m³
 D_d – diameter of downcomer, m
 D_i – diameter of draft tube, m
 D_r – diameter of riser, m
 D_T – diameter of ILBC or NBC, m
 d_p – mean diameter of solid particles, m
 H – Henry's law constant, kmol/Pa · m³
 H_T – static liquid height above gas distributor, m
 H_i – height of draft tube, m
 K – fluid consistency index, Pa · sⁿ
 k_L – gas-liquid oxygen transfer coefficient, m/s
 $k_L a$ – volumetric gas-liquid oxygen transfer coefficient based on dispersion volume, 1/s
 $k_L a_L$ – volumetric gas-liquid oxygen transfer coefficient based on total liquid volume, 1/s
 n – flow behavior index, –
 P_b – oxygen partial pressure at column bottom, Pa
 t – time, s
 U_G – superficial gas velocity, m/s
 U_L – superficial liquid or slurry velocity in riser, m/s
 V_d – liquid volume in downcomer including column top and bottom, m³
 V_r – liquid volume in rise, m³

Greek letters

- γ – average shear rate (= 5000 U_G), 1/s
 ε_G – gas holdup
 ε_S – solid holdup

- μ_a – apparent liquid viscosity (= $K\gamma^{n-1}$), Pa · s
 ρ_S – density of solid particles, kg/m³

Subscripts

- cal. – calculated value
 obs. – observed value

List of abbreviations

- ELBC – external loop airlift bubble column
 GB – glass beads
 ILBC – internal loop airlift bubble column
 IR – ion exchange resin
 NBC – normal bubble column

References

1. Chisti, M. Y., *Airlift bioreactors*. Elsevier Applied Science, New York, NY (1989).
2. Nakao, K., Suenaga, S., Takeda, K., Kimura, M., Robinson, C. W., "Mass Transfer in a Bubble Column with External Liquid Circulation" Preprints of 1st German-Japanese Symp. Bubble Columns, Schwerte, Germany, June 13-15, 1988, p.153-158.
3. Popovic, M., Robinson, C. W., *AIChEJ.* **35** (1989) 393.
4. Douek, R. S., Livingston, A. G., Johansson, A. C., Hewitt, G. F., *Chem. Eng. Sci.* **49** (1994) 3719.
5. Merchuk, J. C., *Can. J. Chem. Eng.* **81** (2003) 324.
6. Nakao, K., Azakami, F., Furumoto, K., Yoshimoto, M., Fukunaga, K., *Can. J. Chem. Eng.* **81** (2003) 444.
7. Nakanoh, M., Yoshida, F., *Ind. Eng. Chem. Process Des. Dev.*, **22** (1983) 577.
8. Lewis, D. A., Davidson, J. F., *Chem. Eng. Sci.* **40** (1985) 2013.
9. Nakao, K., Takeuchi, H., Kataoka, H., Kaji, H., Otake, T., Miyauchi, T., *Ind. Eng. Chem. Process Des. Dev.* **22** (1983) 577.
10. Nishikawa, M., Kato, H., Hashimoto, K., *Ind. Eng. Chem. Process Des. Dev.* **16** (1977) 133.
11. Koide, K., Horibe, K., Kawabata, H., Ito, S., *J. Chem. Eng. Jpn* **18** (1985) 248.
12. Koide, K., Takazawa, A., Komura, M., Matsunaga, H., *J. Chem. Eng. Jpn* **17** (1984) 459.
13. Gourich, B., Azher, N. E., Bellhaj, M. S., Delmas, H., Bouzidi, A., Ziyad, M., *Chem. Eng. Proc.* **44** (2005) 1047.
14. Akita, K., Yoshida, F., *Ind. Eng. Chem. Process Des. Dev.* **13** (1974) 84.
15. Vandu, C. O., Ellenberger, J., Krishna, R., *Chem. Eng. Sci.* **59** (2004) 4999.
16. Akita, K., Yoshida, F., *Ind. Eng. Chem. Process Des. Dev.* **12** (1973) 76.
17. Oliveira, M. S. N., Ni, X. W., *Chem. Eng. J.* **99** (2004) 59.
18. Yoshimoto, M., Suenaga, S., Furumoto, K., Fukunaga, K., Nakao, K., *Proceedings of The 9th Asian Conference on Fluidized-Bed and Three-Phase Reactors, "Gas-Liquid Interfacial Area, Bubble Size and Liquid-Phase Mass Transfer Coefficient in a Three-Phase External Loop Airlift Bubble Column"* Pacific Green Bay, Wanli, Taiwan, November 21-24, 2004, 289-294.

